RSC Advances

PAPER

View Article Online
View Journal | View Issue

Cite this: *RSC Adv.*, 2024, **14**, 24352

Ultrasound assisted efficient separation of lithium from brine with a composite polyether sulfone-ionic liquid membrane

Milad Hermani,[b] Behrang Golmohammadi[a] and Hemayat Shekaari *[a]

Green, selective and efficient extraction of lithium as one of the most important components for energy storages with ultrasound-assisted membrane separation of lithium from brine, which contains alkali metal chlorides, is conducted using a composite membrane. The composite membrane is formed by sealing a supported ionic liquid membrane (consisting of 1-alkyl-3-methylimidazolium hexafluorophosphate ([RMIM][PF_6]) + TBP) with a polyethersulfone (PES) membrane and a PVC thin film membrane. The aim of the study is to optimize the separation process for the selective extraction of lithium from alkali metals. Various parameters, including membrane composition, feed concentration, and ultrasonic conditions, are adjusted to identify the best operating conditions. The results reveal that a membrane containing xIL = 0.5 of [MOIM][PF_6] exhibits higher selectivity compared to other membranes studied. The flux of lithium initially increases with shorter sonication times, but it decreases as the duration of ultrasonic irradiation is prolonged. The optimal frequency for the ultrasonic treatment, which matches the bulk modulus of the membrane, is approximately 250 kHz. Higher frequencies result in higher flux and selectivity in lithium separation; besides, optimizing the amplitude and pulse cycle of the ultrasound at 75% leads to increased flux. Moreover, higher flux and selectivity (percentage of lithium with respect to the all of the ion flux) are achieved when separating lithium from alkali metal chlorides at higher feed concentrations, ranging from 250 ppm to 1000 ppm. The selectivity is influenced by the hydrophobicity, which depends on the behavior of the ionic liquid membrane. The process is promising for the future of the lithium mining from brine.

Received 30th May 2024
Accepted 22nd July 2024

DOI: 10.1039/d4ra03986f

rsc.li/rsc-advances

1. Introduction

Lithium extraction methods vary depending on the source and geological characteristics of the deposits.[1,2] Hard rock mining involves excavating ore bodies to extract lithium-bearing minerals, while brine extraction involves pumping naturally occurring lithium-rich brines from underground reservoirs and concentrating the lithium through solar evaporation.[3] Geothermal extraction utilizes lithium-bearing brines from geothermal energy production, and clay extraction employs leaching techniques to extract lithium from clay minerals such as hectorite and jadarite.[2,4,5]

Various green methods for separation are applied while ionic liquids membranes are one of the emerging methods with high capability.[6] Also, different polymeric membranes have been developed for separation of lithium from brine.[7] Lithium separation can be achieved using various membranes, including polyether sulfone (PES) membranes and supported ionic liquid membranes (SILMs).[8] PES membranes excel in chemical resistance, mechanical strength, and thermal stability, making them suitable for electrodialysis, nanofiltration, and ultrafiltration applications.[9] SILMs, on the other hand, offer high selectivity for lithium ions and can be tailored to specific applications.[10–17]

Ultrasonic waves play a crucial role in enhancing mass transfer and membrane cleaning in lithium separation processes. Acoustic cavitation, induced by ultrasonic waves, creates turbulence and microstreaming, increasing mass transfer rates.[18] Additionally, ultrasonic waves dislodge foulants from membranes, extending their lifespan and improving performance. Acoustic waves propagating through membranes generate pressure fluctuations, particle displacement, and acoustic particle velocity.[19] The acoustic wave equation describes the pressure variations caused by ultrasonic waves, while the diffusion equation governs the flux of permeated ions based on concentration gradients.[20] These equations provide fundamental insights into the interactions between ultrasonic waves and membranes in lithium separation processes.

The extraction of lithium from various sources necessitates careful selection of extraction methods and membranes. Ultrasonic waves offer significant benefits in enhancing mass

[a]Department of Physical Chemistry, Faculty of Chemistry, University of Tabriz, Tabriz, 5166616471, Iran. E-mail: hemayatt@yahoo.com
[b]Department of Chemical Engineering, Amirkabir University of Technology (Tehran Polytechnic), Hafez Ave, P.O. Box 15875-4413, Tehran, Iran

transfer and membrane cleaning, while acoustic waves and diffusion equations provide theoretical underpinnings for membrane processing. In the present work, a series of composite membranes containing ionic liquid membranes impregnated into the PES membranes has been used to separate lithium from the brine containing alkali metals ions with an ultrasonic assisted process.

2. Theoretical background

Our previous research show that the ILMs are potential for fast and selective separation of lithium from the alkali metals brine by assistance of ultrasonic propagation.[18] The sound pressure is a complex variable that depends on time and position. The analytical expressions for the pressure could be evaluated through a physical-mathematical process in one dimension. The particle displacement (ξ), particle velocity (v), ultrasonic pressure (p), and the pressure difference in two side of membrane (Δp) caused by ultrasonic propagation are described by the following equations:[21–23]

$$\xi^{+}(x,t) = h(ut - x) \quad (1)$$

$$v^{+}(x,t) = h'u \quad (2)$$

$$p^{+}(x,t) = \gamma P_0\left(\frac{\partial \xi}{\partial x}\right) = h'\rho u^2 \quad (3)$$

$$\Delta p = 2\rho f A \mu \quad (4)$$

where, u is the speed of sound and h represents the direction vector of the sound propagation. This equation relates the pressure amplitude (ΔP) generated by the ultrasonic wave to the density of the medium (ρ), the frequency of the ultrasound wave (f), the amplitude of the wave (A), and the displacement of the membrane (μ). According to the previous experiments this principles are justified for ILM containing 1-butyl-3-methylimidazolim hexafluorophosphate and tributyl phosphate for alkali metal separation from aqueous media.[18] However, the selectivity of the lithium was not investigated in the presence of other alkali metals. Also, there is a potential of dispersion of the ILM in the feed phase and formation of the emulsion liquid membrane in the feed phase besides the thickness of the ILM was high that limits the metal ion flux through the membrane. Impregnation of the ILM into a polymeric porous membrane has been used to avoid and overcome these obstacles. In this respect, PSF substrate has been impregnated with different ILMs such as 1-alkyl-3-methylimidazolium hexafluorophosphate (alkyl = butyl, hexyl, octyl) in the presence of tributyl phosphate with different compositions of these ILMs.

3. Materials and methods

3.1. Materials

Polyether sulfone granule, polyvinylchloride, and polyvinylpyrrolidone have been supplied by Merck. Also, the 1-methylimidazole, *N*-methyl-2-pyrrolidone, 1-butyl chloride, 1-hexyl chloride, octyl chloride, potassium hexafluorophosphate, and tributyl phosphate, tetrahydrofuran, ethyl acetate, *N*-hexane besides the utilized salts including LiCl, NaCl, and KCl have been purchased from Merck. Deionized water with specific conductance below 1 $\mu S\ cm^{-1}$ have been used for preparation of aqueous solutions.

3.2. Membrane casting

3.2.1. Polymer and solvent preparation. PES polymer (5 wt%) was accurately weighed using a digital weighing balance. In a glass beaker, the PES polymer was dissolved in NMP solvent under constant stirring using a magnetic stirrer until a homogeneous polymer solution was obtained. The PVP pore-forming agent (10 wt% relative to the PES polymer) was prepared separately by dissolving 2wt% PVP in NMP, followed by stirring until complete dissolution.

3.2.2. Membrane casting. A clean glass substrate was placed on a level surface. The PES/NMP polymer solution was poured onto the glass substrate. Using a stainless-steel casting knife with a thickness of 100 micrometers, the polymer solution was spread evenly on the glass substrate to achieve the desired thickness. The casting knife was held at a consistent angle, and a gap of 100 micrometers was maintained between the blade and the glass substrate. The casting knife was moved at a steady speed of 2 centimeters per second to ensure uniform membrane formation. Immediately after spreading the polymer solution, the PVP pore-forming agent solution was applied on top of the polymer layer using a dropper, ensuring even distribution over the entire surface. The PVP solution was allowed to settle for 1 minute to facilitate pore formation. The glass substrate with the casted membrane was carefully transferred into a water bath maintained at 25 °C. The membrane was left in the water bath for 1 hour to allow for coagulation and solidification. Gentle agitation of the water bath was performed to aid the coagulation process. After coagulation, the membrane was carefully removed from the water bath and rinsed with distilled water to remove residual NMP and PVP. The rinsing process was repeated three times to ensure thorough cleaning. The washed membrane was placed in a drying oven at 60 °C for 24 hours to remove any remaining water and residual solvent.

3.2.3. Synthesis of the ionic liquids. A two-step synthesis method has been utilized for preparation of the ionic liquids including direct alkylation of 1-methylimidazole with chloroalkane to from 1-alkyl-3-methylimidazolium chloride, and anion exchange reaction with potassium hexafluorophosphate for replacing chloride with hexafluorophosphate as reported in previous work. The rout of synthesis is given in Scheme 1.

3.2.4. Preparation of ionic liquid membrane. A series of ionic liquid membrane including 1-alkyl-3-methylimidazolium hexafluorophosphate (alkyl = butyl, hexyl, octyl) + tributyl phosphate (TBP) as carrier with different composition of IL/TBP has been prepared as our previous work. Briefly, an analytical balance (AND, GR202) has been used for weighing of ILs and TBP in gas tight bottles and stirred for 30 min and sonicated for 10 min to prepare different concentration of ILM. It should be

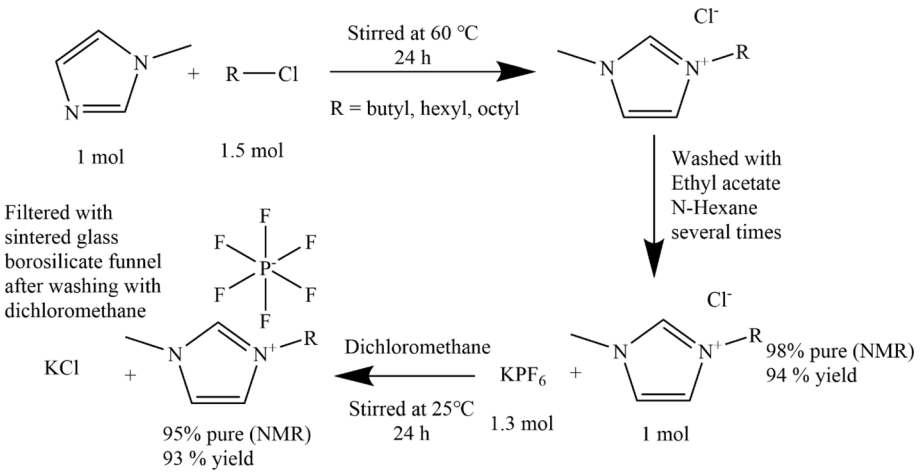

Scheme 1 The rout of synthesis of 1-alkyl-3-methylimidazolium hexafluorophosphate.

noted that in the concentrated IL region it might take longer sonication to degas the ILM.

3.2.5. Preparation of supported ionic liquid membranes. A multi layered complex membrane has been prepared including PES as main substrate, {1-alkyl-3-methylimidazolium hexafluorophosphate (alkyl = butyl, hexyl, and octyl) + tributyl phosphate} as ionic liquids membrane, and porous PVC membrane (PVP dopped as creator of pores) as inlet and outlet layer of the PES supported ionic liquid membrane. The supported ionic liquid has been prepared with immersing of the PES membrane in different composition (weight fraction) of the ILM {(IL + TBP)/(25 : 75), (50 : 50), (75 : 25)} for 24 h, then the membrane has been cleaned on the cellulose acetate filters to remove excess amount of the ILM, and vacuumed for 30 min in a dead-end module as given in Scheme 2 to place the ILM inside the PES pores and achieve an integral and uniform membrane phase.

3.2.6. Preparation of complex multilayer supported ionic liquid membrane. A polymeric solution including 1 g PVP as pore former in (4 g PVC + 10 g THF) has been prepared by stirring it for 24 h at room temperature in a gas tight autoclave bottle to seal THF leaking. After sonication for 1 h for removing bubbles formed in solution, the solution cooled down to room temperature, and the solution has been applied on the supported ILM (IL + PES sheet) and sealed with dip coating and dried in air for 5 min to evaporate THF. After this process a complex supported ILM with porous PVC membrane was formed that have been characterized with FESEM with corresponding thickness of each layer of synthesized complex membrane.

3.3. Characterization of the prepared membranes

The prepared membranes surface and cross section have been characterized with field emission scanning electron microscopy (TESCAN, MIRA3 FEG-SEM). A sheet with dimension of 2 × 1 cm^2 from the prepared membranes have been soaked into the liquid nitrogen for several minutes and were broken that is used for the cross-sectional images.

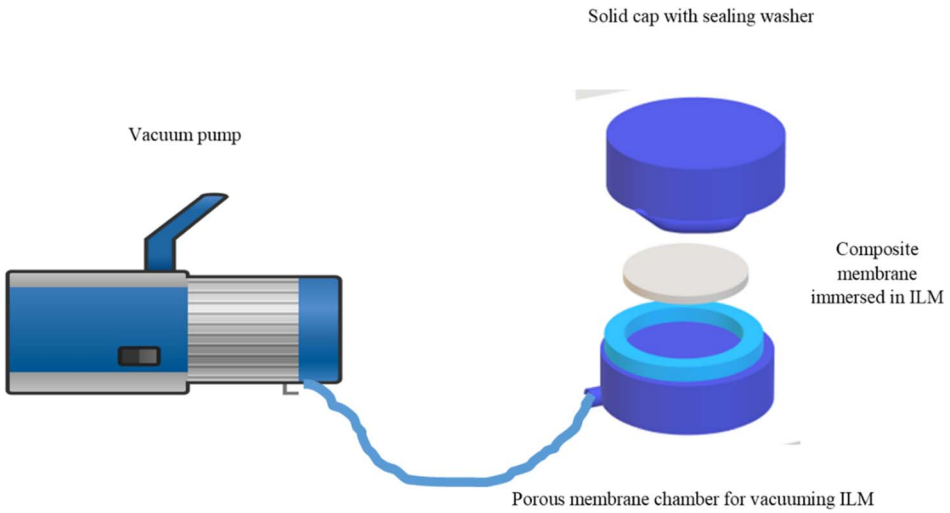

Scheme 2 Module for fast impregnation of ILM into the polymeric membrane.

3.4. Feed phase

The feed phase has been prepared according to our previous experience. The separate feeds have been studied in the previous work with ILM membrane containing just one alkali metal ions and it has been found that the ultrasonic assisted liquid membrane could be very efficient. According to the experience in this work a mixture of alkali metals have been prepared that include 250, 500, 750, and 1000 ppm of Li^+, Na^+, and K^+ ions with chloride anion to reduce the interference of the anion effect in the determination of the alkali content.

3.5. Ultrasonic assisted selective separation of lithium from alkali metal ion aqueous mixture

Different complex membranes have been synthesized according to the procedure mentioned earlier and utilized for separation alkali metals ions from a simulated brine feed containing lithium, sodium, and potassium chloride. An ultrasonic probe (Dr Heilsher, GmbH, UP-400, ultraschall-processor) is used to produce mechanical sound waves with considerably local high pressure as driving force in the membrane separation. The utilized setup sketch design has been illustrated in Scheme 3.

The two container of the feed and receiving phases was made of glass while the silicon washers was used for sealing of the of these flanged tubes. A valve has been used for charge and discharge of the receiving phase. The utilized setup technical information is clearly illustrated in the Scheme 1. The effect of different factors in the separation process of Li from the Na and K such as frequency, amplitude, and sonication pulse sequence, sonication time and feed phase composition has been studied.

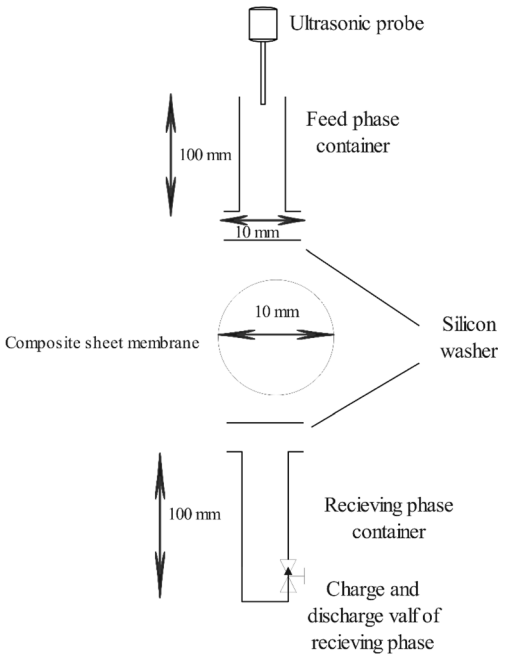

Scheme 3 The sketch design of the setup used as membrane module for Li separation from simulated alkali metal brine with composite ionic liquid membrane.

3.6. Analysis of receiving phase alkali metal content

A flame photometer (Jenway, PFP7) has been used to analyze the content of the alkali metals in the receiving phase after sonication process. It should be noted that the standards have been used for calibration of the instrument were clinical dilute standards (10 ppm) to reduce the interference of different alkali metal contents.

4. Results and discussion

A series of composite membranes including PES membrane impregnated with ILM ([BMIM][PF_6], [HMIM][PF_6], [MOIM][PF_6], and TBP) with different weight fraction of the ILs and sealed with PVC thin film membranes (PVC as base and PVP as pore former) have been fabricated and characterized. An array of experiments was conducted under atmospheric pressure and at room temperature (298.15 K) to assess the capabilities of the separation system. The ultrasound at different frequencies, separation times, amplitude of the ultrasonic, ultrasonic pulse sequence percentage, and feed phase concentrations including 250–1000 ppm of Li^+, Na^+, and K^+ have been investigated to achieve the best condition for efficient Li^+ separation. It should be noted that the ultrasonic pressure on the membrane surface has been estimated to be 3400 $\pm$ 10 Pa.

4.1. Characterization of membranes

4.1.1. Morphology imaging. Fig. 1 and 2 illustrates the cross-sectional and surface field-emission scanning electron microscopy (FESEM) images of the studied membranes. The PES membrane exhibited a finger-like structure with a sponge-like porous body as a characteristic of PES membrane.

A uniform surface has been achieved for the PES with high integrity level on surface that is illustrated in Fig. 1b. A uniform surface with a high level of integrity has been successfully achieved for the polyethersulfone (PES) membrane. Fig. 2 illustrates a three-layer composite membrane structure consisting of a supported ionic liquid membrane (SILM) with a polyether sulfone (PES) substrate. The pores in the membrane were observed to be filled upon impregnation with the ILM. Furthermore, as the alkyl chain length in the IL increased from butyl to octyl, the integrity of the membrane increased, and the pores are filled with ILM. The SILM is sandwiched between two layers of sponge-like thin film PVC membrane. The fabrication process involves dip coating the SILM into a solution of PVC (polyvinyl chloride) and PVP (polyvinylpyrrolidone) in THF (tetrahydrofuran).

Fig. 2b depicts the surface of the thin film PVC membrane, showcasing notable features and characteristics. The surface of the membrane exhibits the formation of semi-circular pores with a diameter of 1 μm. These pores are a result of the rapid evaporation of THF (tetrahydrofuran) during the fabrication process, combined with the presence of PVP (polyvinylpyrrolidone) as a pore-forming agent.

4.1.2. Composite membrane ILM dependent characteristics. The membrane ILM uptake density dependency, loss rate in the presence of the ultrasonic and water contact angle have

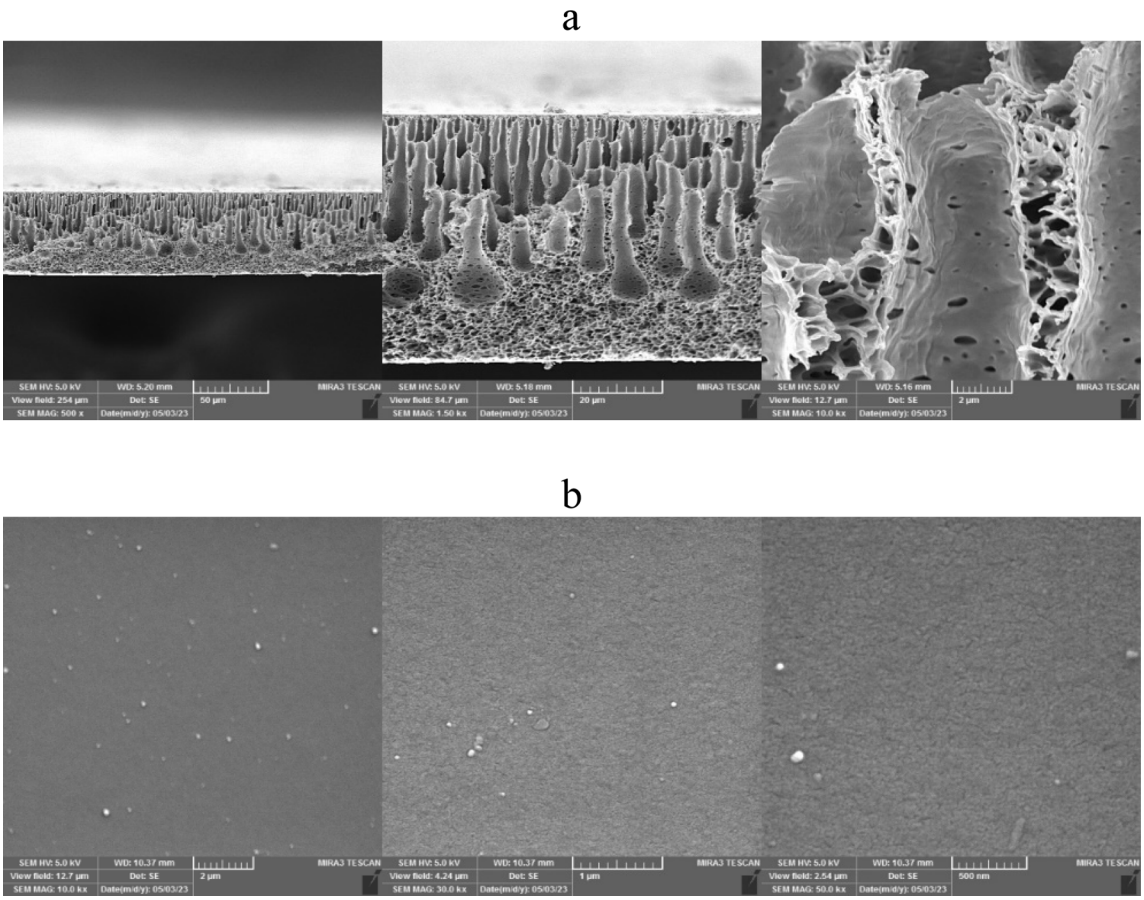

Fig. 1 The FESEM (a) cross-sectional and (b) surface morphology images of the PES membrane.

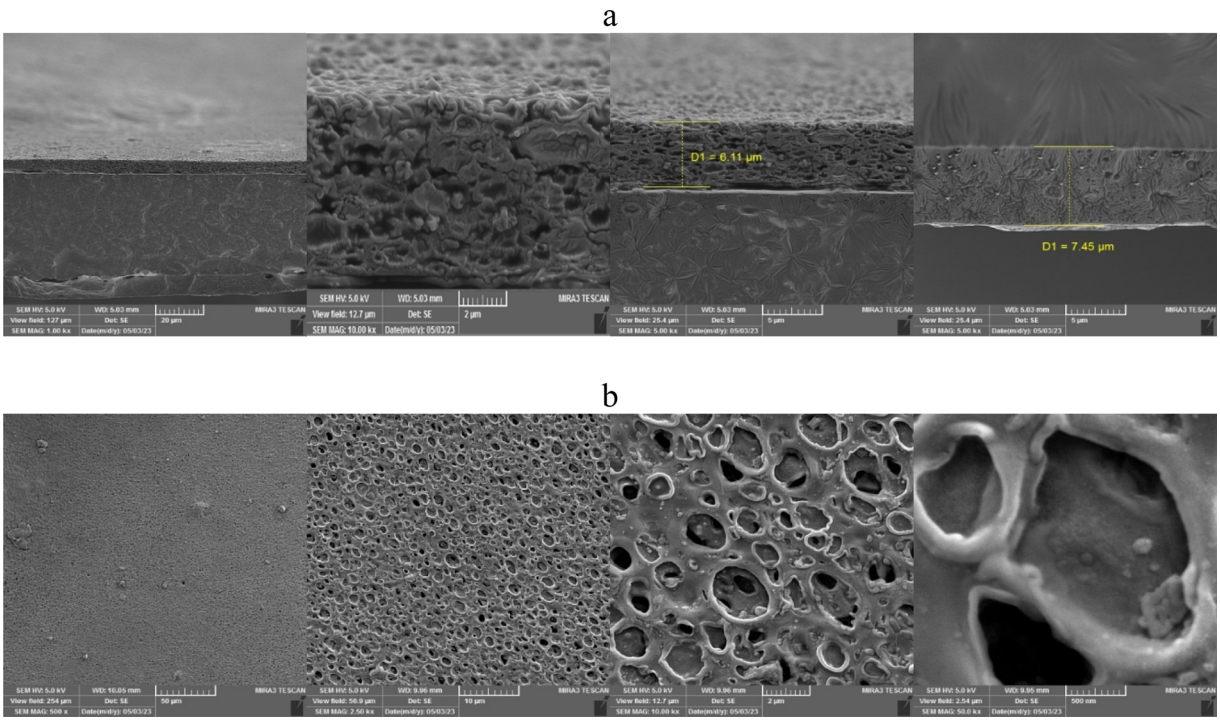

Fig. 2 (a) The cross-sectional FESEM images of composite membranes including impregnated PES membrane with ILM containing [HMIM][PF_6] + TBP with weight fraction of 50 : 50 that has been sealed with PVC thin film membrane (b) the FESEM images from sealing PVC thin film membrane.

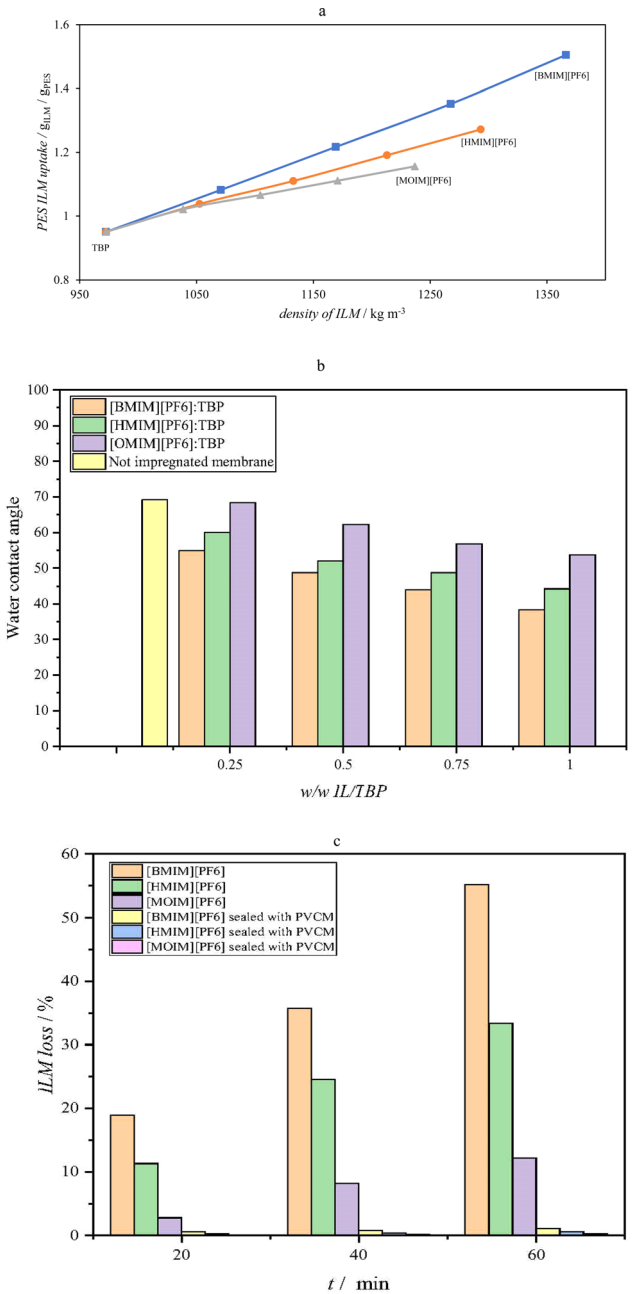

Fig. 3 a) Density dependency of PES membrane ILM uptake (b) ILM loss in the presence of ultrasonic irradiation for the supported ionic liquid with and without PVCM sealing, and (c) effect of ILMs weight fraction in the presence of TBP on the water contact angle of impregnated PES membrane.

been illustrated in Fig. 3. The increased density of the ILM lead to increase in the ILM uptake by PES.[24] Obviously, membrane with higher density would be filled more as the membrane porosity is constant.

The hydrophobic PES membrane effectively interacts with hydrophobic ILs due to its higher density, providing more sites for the ILs for adhering.[25] This hydrophobic interaction further enhances the uptake of ILs into the membrane. The water contact angle has been recorded 69.27° and 76.33° for PVC and PES membranes sheets, respectively. Solvation of the ILs in alkaline solution is inevitable, but the proposed methods, including adding a slating-out agent, are not the most efficient in preventing IL loss.[18] Instead, a sealing membrane containing a porous PVC membrane with PVP as a pore-former has been shown to significantly reduce IL loss. This is because the hydrophobic PVC membrane limits water access to the ILs, while its porosity allows for alkaline solution transfer, reducing IL loss.[26] The viscosity or rheological properties of the ILs are not the main factor influencing IL loss. Impregnation of ILs into the PES membrane decreases its water contact angle, indicating enhanced hydrophilicity. This is attributed to various interactions, including hydrogen bonding, dipole–dipole interactions, ion–dipole interactions, and surface modification. The combined effect of these interactions is responsible for the observed hydrophilicity pattern of the impregnated PES membranes.[27]

4.2. Separation of alkali chloride salts with ultrasound assisted membrane processing

In order to harness the power of ultrasonic pressure as a driving force, it becomes imperative to channelize sound waves effectively. To fulfill this requirement, a flanged glass tube with a 10 mm internal diameter was employed. This choice proved suitable for the ultrasonic probe and its narrow dimensions effectively minimized issues such as refraction, reflection, and diffraction of the propagating sound waves. The frequency range selected for these experiments was between 50 to 250 kHz, ensuring that the ultrasound waves did not experience significant attenuation while passing through the osmosis tube.[28] Also different sequence percentage and amplitude of the ultrasonic has been adjusted to 25–75% for investigation of these variables affect. Feed phase was prepared by 250–1000 ppm of Li^+, Na^+, K^+ with chloride anion. Since during sonication significant amount of heat was created in the media, the sonication time was selected as short as possible in a range of 60–300 s.

4.2.1. Effect of ultrasonic parameters in separation

4.2.1.1. Effect of frequency. The effect of frequency of ultrasonic on the flux of alkali metals through the fabricated composite membranes have been calculated for different variety of experiment conditions and the results are given in Table 1. According to the results of this table, the increasing frequency led to increase in the total flux while lithium increment is significantly higher than sodium and potassium. Also, this trend completely has been shown in Fig. 4a. As results suggests, the selectivity of the process to the lithium has been increased by increasing of the frequency and this effect is stronger for [OMIM][PF_6] rather than other two ionic liquids and the ILM concentration led to improve selectivity while the flux of the content is decreased at higher concentration of the IL.

When the sound frequency matches the membrane's resonance frequency, it can cause acoustic resonance, enhancing permeability.[29] High-frequency sound waves can damage the membrane and reduce permeability. The membrane's response to pressure varies with frequency, being more elastic at lower

Table 1 Effect of frequency with different composite membrane containing supported ILM in PES sealed in PVC thin film membrane with a 120 s sonication time, 50% amplitude and sonication sequence pulse with a feed phase concentration containing 500 ppm of chlorine slats of Li, Na, and K in the presence of different concentration of ILM

f (kHz)	J_{Li} (mg cm^{-2})	J_{Na} (min^{-1} Pa^{-1})	J_K	J_t	S (%)
[BMIM][PF$_6$]					
xIL = 0.25					
50	2.28	0.28	0.05	2.52	90.50
100	7.18	0.28	0.05	7.42	96.78
150	10.83	0.40	0.02	11.21	96.63
250	11.98	0.31	0.04	12.33	97.18
xIL = 0.50					
50	3.39	0.26	0.05	3.71	91.59
100	9.24	0.31	0.04	9.59	96.38
150	12.00	0.40	0.02	12.42	96.59
250	12.98	0.45	0.01	13.45	96.53
xIL = 0.75					
50	1.91	0.11	0.03	2.05	92.98
100	6.50	0.28	0.05	6.83	95.18
150	9.56	0.28	0.05	9.89	96.67
250	10.66	0.31	0.04	11.01	96.85
[HMIM][PF$_6$]					
xIL = 0.25					
50	2.85	0.23	0.06	3.14	90.88
100	8.14	0.23	0.06	8.43	96.60
150	12.05	0.31	0.04	12.39	97.20
250	13.68	0.18	0.06	13.93	98.24
xIL = 0.50					
50	4.39	0.16	0.04	4.59	95.63
100	10.61	0.21	0.06	10.87	97.58
150	13.99	0.35	0.03	14.38	97.30
250	14.85	0.38	0.03	15.26	97.34
xIL = 0.75					
50	2.55	0.09	0.02	2.66	95.84
100	7.82	0.18	0.06	8.07	96.96
150	10.24	0.21	0.06	10.50	97.50
250	11.78	0.18	0.06	12.03	97.96
[MOIM][PF$_6$]					
xIL = 0.25					
50	2.70	0.10	0.01	2.81	96.11
100	8.62	0.10	0.01	8.72	98.75
150	12.35	0.15	0.01	12.51	98.70
250	10.93	0.10	0.01	11.04	99.01
xIL = 0.50					
50	4.66	0.08	0.02	4.75	98.03
100	11.67	0.10	0.01	11.78	99.07
150	14.46	0.16	0.07	14.69	98.45
250	15.36	0.18	0.06	15.60	98.48
xIL = 0.75					
50	3.75	0.02	0.03	3.80	98.77
100	8.40	0.09	0.01	8.50	98.81
150	11.08	0.10	0.01	11.19	99.02
250	12.82	0.10	0.01	12.93	99.15

frequencies and more viscoelastic at higher frequencies.[30] Factors like internal friction and molecular relaxation processes can decrease the membrane's bulk modulus at high frequencies. The specific behavior depends on material, temperature, pressure, and composition. Polyethersulfone (PES) membranes are elastic at low frequencies but exhibit a decrease in bulk modulus at higher frequencies due to viscoelasticity. Polyvinyl chloride (PVC) membranes with polyvinylpyrrolidone (PVP) as a pore former show similar behavior. Frequency-dependent effects are influenced by factors like PVP concentration, thickness, and processing conditions.

4.2.1.2. Effect of amplitude. Effect of amplitude of the ultrasonic wave have been studied and the results are collected in Table 2 for a condition of 120 s sonication time, 100 kHz frequency and 50% sonication sequence pulse with a feed phase concentration containing 500 ppm of chlorine slats of Li, Na, and K. The variation of the alkali metals flux with amplitude of the ultrasonic wave has been given in Fig. 4b for membrane containing 0.5 weight fraction of [MOIM][PF$_6$] besides an schematic indicating effect of amplitude on membrane. The amplitude raising has an increasing effect for larger particles while it reaches to maximum in 50% of amplitude for the smaller particle (Li) and increases the selectivity of membrane for Li. Amplitude in waves refers to their magnitude or size, measuring how much they deviate from their equilibrium position. It affects energy, intensity, and perception. Higher amplitude means more energy, louder sounds, and brighter light. Frequency, the number of oscillations per unit time, influences pitch and color. In summary, amplitude plays a crucial role in determining wave behavior and our sensory experiences.

For each ILM type (*e.g.*, [BMIM][PF$_6$], [HMIM][PF$_6$], [MOIM][PF$_6$]), the flux and selectivity change with different concentrations (xIL). Higher ILM concentration generally leads to increased flux but may impact selectivity. The specific trends depend on the ILM type and concentration. In summary, this study investigates how different composite membranes with supported ILM perform in terms of ion flux and selectivity under specific sonication conditions and feed phase compositions. The effect of ultrasonic amplitude on separation varies depending on factors such as the separation process and component properties. Higher ultrasonic amplitudes increase mechanical agitation and mixing, enhancing component contact and facilitating separation.[31] These higher amplitudes create strong pressure variations and disrupt concentration gradients near the membrane surface through acoustic streaming.[32] This disruption helps overcome diffusion limitations, resulting in more efficient separation.[33] Higher ultrasonic amplitudes also promote mass transfer across the separation interface.[34] However, excessively high amplitudes can damage or deform the membrane, reducing separation efficiency. Therefore, it's crucial to consider the mechanical properties and limitations of the membrane material when determining the appropriate ultrasonic amplitude.[35] Generally, there exists an optimal range of ultrasonic amplitudes for the best separation performance, ensuring effective mixing and mass transfer without excessive damage to the membrane or other components. In our case, an amplitude of 50% was found to provide higher selectivity for Li, making it the best operating condition.

4.2.1.3. Effect of pulse sequence. Ultrasonic pulse sequence effect on the flux of alkali metals through the fabricated membranes has shown in Table 3. A comparative result for 3 different membranes with 0.5 weight fraction of the ILs shows

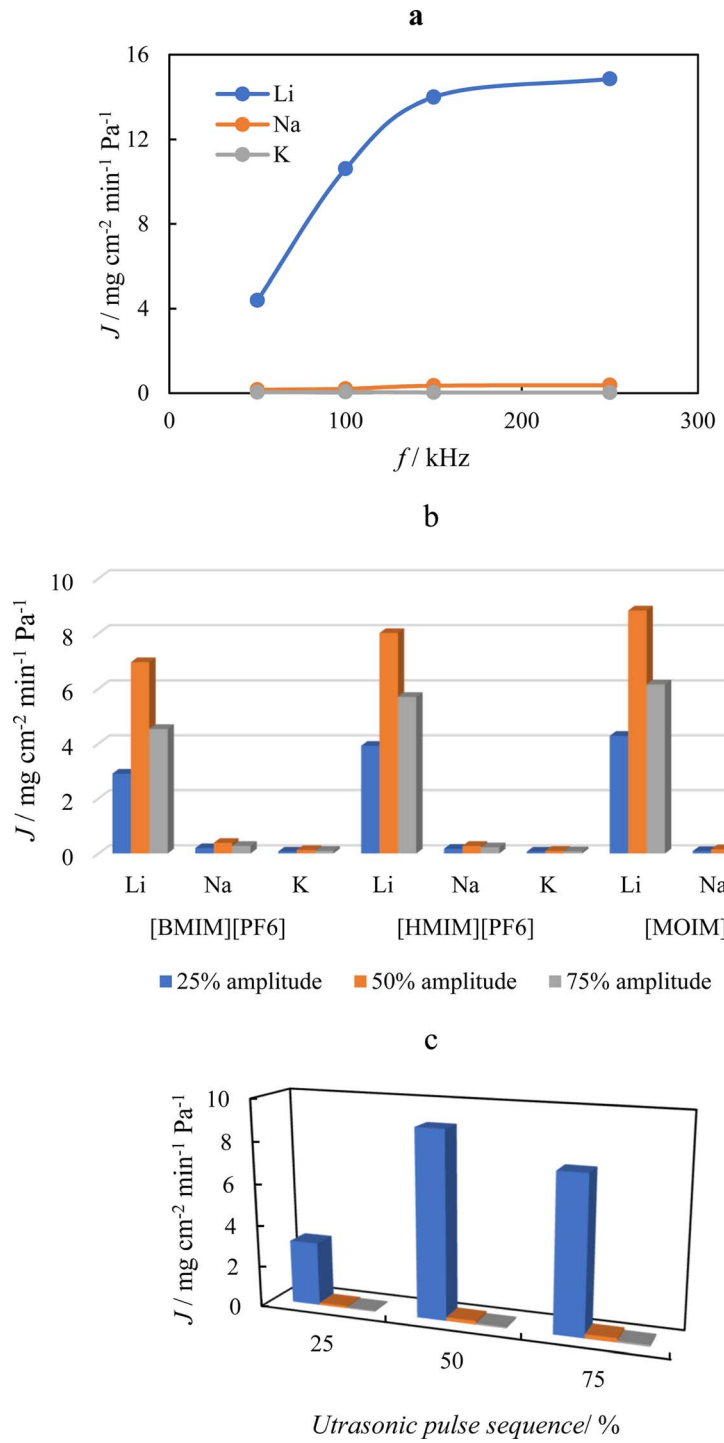

Fig. 4 (a) The effect of ultrasonic frequency on flux of Li, Na, K through the composite membrane containing 0.5 weight fraction [HMIM][PF_6] in PES sealed in PVC thin film membrane with a 120 s sonication time, 50% amplitude and sonication sequence pulse with a feed phase concentration containing 500 ppm of chlorine slats of Li, Na, and K. (b) Flux variation with amplitude with condition of 120 s sonication time, 100 kHz frequency and 50% sonication sequence pulse with a feed phase concentration containing 500 ppm of chlorine slats of Li, Na, and K for the composite membrane containing 0.5 weight fraction of the ILs. (c) Comparison of flux of alkali metals through fabricated membranes with the sonication pulse sequence with 0.5 weight fraction of [MOIM][PF_6] under a condition with 120 s sonication time, 100 kHz frequency and 50% amplitude with a feed phase concentration containing 500 ppm of chlorine slats of Li, Na, and K.

that the permeate flux was increased by increment of the pulse sequence percentage from 25% to 50% while it is decreased from 50% to 75%. Also, it is shown that [OMIM][PF_6] has more flux rate between the studied ILs with higher selectivity ratio. The effect of sonication pulse sequence on the separation of lithium (Li) from other alkali metals (sodium, Na, and

Table 2 Effect of amplitude% with different composite membrane containing supported ILM in PES sealed in PVC thin film membrane with a 120 s sonication time, 100 kHz frequency and 50% sonication sequence pulse with a feed phase concentration containing 500 ppm of chlorine slats of Li, Na, and K in the presence of different concentration of ILM

A (%)	J_{Li} (mg cm^{-2})	J_{Na} (min^{-1} Pa^{-1})	J_K	J_t	S_{Li} (%)
[BMIM][PF$_6$]					
xIL = 0.25					
25	1.66	0.27	0.10	2.03	81.68
50	5.50	0.39	0.12	6.02	91.47
75	4.05	0.30	0.11	4.45	90.87
xIL = 0.50					
25	1.94	0.25	0.09	2.28	85.24
50	7.09	0.42	0.13	7.64	92.82
75	5.39	0.44	0.14	5.97	90.23
xIL = 0.75					
25	1.33	0.17	0.07	1.57	84.78
50	4.98	0.39	0.12	5.50	90.67
75	3.19	0.22	0.08	3.49	91.38
[HMIM][PF$_6$]					
xIL = 0.25					
25	2.14	0.19	0.08	2.41	88.63
50	6.25	0.33	0.11	6.68	93.51
75	4.74	0.22	0.08	5.04	94.03
xIL = 0.50					
25	2.79	0.19	0.08	3.06	91.04
50	8.14	0.30	0.11	8.55	95.24
75	6.52	0.39	0.12	7.03	92.70
xIL = 0.75					
25	1.77	0.14	0.06	1.98	89.70
50	6.00	0.27	0.10	6.37	94.17
75	3.97	0.17	0.07	4.21	94.32
[MOIM][PF$_6$]					
xIL = 0.25					
25	2.02	0.11	0.05	2.19	92.31
50	6.61	0.18	0.07	6.86	96.39
75	5.18	0.13	0.06	5.37	96.38
xIL = 0.50					
25	3.07	0.10	0.05	3.23	95.07
50	8.96	0.18	0.07	9.21	97.31
75	7.45	0.20	0.08	7.74	96.34
xIL = 0.75					
25	2.83	0.08	0.05	2.95	95.79
50	6.44	0.17	0.07	6.68	96.42
75	4.45	0.10	0.05	4.60	96.73

Table 3 Effect of sonication sequence pulse% with different composite membrane containing supported ILM in PES sealed in PVC thin film membrane with a 120 s sonication time, 100 kHz frequency and 50% amplitude with a feed phase concentration containing 500 ppm of chlorine slats of Li, Na, and K in the presence of different concentration of ILM

Sonication pulse sequence (%)	J_{Li} (mg cm^{-2})	J_{Na} (min^{-1} Pa^{-1})	J_K	J_t	S_{Li} (%)
[BMIM][PF$_6$]					
xIL = 0.25					
25	2.05	0.22	0.08	2.35	87.08
50	5.37	0.36	0.12	5.85	91.82
75	3.88	0.20	0.07	4.15	93.53
xIL = 0.50					
25	2.90	0.20	0.07	3.17	91.54
50	6.96	0.39	0.13	7.47	93.12
75	4.53	0.28	0.10	4.90	92.38
xIL = 0.75					
25	1.45	0.17	0.07	1.69	85.66
50	4.85	0.36	0.12	5.33	91.02
75	3.02	0.15	0.06	3.23	93.58
[HMIM][PF$_6$]					
xIL = 0.25					
25	2.70	0.15	0.06	2.90	92.86
50	6.12	0.30	0.10	6.51	93.86
75	4.65	0.22	0.08	4.95	93.87
xIL = 0.50					
25	3.92	0.17	0.07	4.16	94.17
50	8.01	0.28	0.10	8.39	95.54
75	5.70	0.22	0.08	6.00	94.94
xIL = 0.75					
25	2.14	0.15	0.06	2.34	91.16
50	5.87	0.25	0.09	6.21	94.54
75	3.92	0.12	0.05	4.09	95.79
[MOIM][PF$_6$]					
xIL = 0.25					
25	2.87	0.08	0.04	2.99	95.71
50	6.48	0.15	0.06	6.70	96.77
75	5.14	0.09	0.04	5.28	97.40
xIL = 0.50					
25	4.28	0.08	0.04	4.41	97.09
50	8.83	0.15	0.06	9.05	97.61
75	6.15	0.12	0.05	6.33	97.28
xIL = 0.75					
25	3.11	0.07	0.04	3.22	96.56
50	6.31	0.15	0.06	6.52	96.82
75	4.61	0.06	0.04	4.70	98.02

potassium, K) using composite membranes containing supported ionic liquid membrane (ILM) reveals that certain composite membranes, particularly those with xIL = 0.5, exhibit high Li^+ selectivity over Na^+ and K^+.

Ultrasonic waves applied to a membrane can enhance permeate flux by inducing cavitation, generating shear forces, disrupting concentration polarization, and loosening blocked pores.[36] The specific effects depend on the membrane type, feed solution characteristics, and operating conditions.[37] Incrementing the ultrasonic pulse sequence further enhances these mechanisms, leading to a substantial increase in permeate flux. Comparative diagrams of flux of Li, Na, and K have been given in Fig. 4c.

4.2.1.4. Effect of sonication time. Efficiency in a separation process heavily relies on time. The impact of time was examined in comparison to a concentration gradient and ultrasonic treatment for separating alkali chloride metals. Both the concentration gradient and ultrasonic treatment were investigated. The analysis of the results showed that the concentration gradient method using the studied ILM achieved a separation of lithium about 20 ppm after 5 hours. The results of the sonication time are given in Table 4. The data provided investigates the impact of sonication time on the separation of lithium (Li) from other alkali metals (sodium, Na, and potassium, K) using composite membranes containing supported ionic liquid

Table 4 Effect of sonication time with different composite membrane containing supported ILM in PES sealed in PVC thin film membrane with a 100 kHz ultrasonic frequency, 50% amplitude and sonication sequence with a feed phase concentration containing 500 ppm of chlorine slats of Li, Na, and K in the presence of different concentration of ILM

t (min)	J_{Li} (mg cm^{-2})	J_{Na} (min^{-1} Pa^{-1})	J_K	J_t	S_{Li} (%)
[BMIM][PF$_6$]					
xIL = 0.25					
1	6.76	0.77	0.26	7.78	86.86
2	5.45	0.45	0.14	6.04	90.18
3	5.64	0.41	0.12	6.17	91.39
4	4.94	0.35	0.10	5.39	91.65
5	4.82	0.34	0.09	5.25	91.83
xIL = 0.50					
1	10.74	0.83	0.28	11.84	90.67
2	7.03	0.48	0.15	7.67	91.73
3	6.14	0.39	0.11	6.64	92.45
4	5.66	0.34	0.10	6.09	92.79
5	5.03	0.35	0.10	5.48	91.79
xIL = 0.75					
1	5.62	0.70	0.24	6.56	85.65
2	4.93	0.45	0.14	5.52	89.26
3	5.07	0.39	0.11	5.57	91.01
4	4.56	0.37	0.11	5.04	90.47
5	4.32	0.35	0.10	4.77	90.56
[HMIM][PF$_6$]					
xIL = 0.25					
1	7.97	0.64	0.23	8.84	90.17
2	6.19	0.39	0.13	6.71	92.23
3	6.05	0.36	0.11	6.52	92.78
4	5.30	0.31	0.09	5.70	93.01
5	5.11	0.27	0.08	5.46	93.63
xIL = 0.50					
1	12.61	0.57	0.21	13.39	94.19
2	8.10	0.35	0.12	8.57	94.51
3	6.94	0.28	0.09	7.31	94.96
4	6.24	0.28	0.08	6.60	94.58
5	5.43	0.27	0.08	5.78	93.99
xIL = 0.75					
1	6.34	0.51	0.20	7.05	89.99
2	5.94	0.32	0.11	6.37	93.26
3	5.51	0.28	0.09	5.88	93.74
4	5.36	0.31	0.09	5.75	93.07
5	4.84	0.27	0.08	5.18	93.29
[MOIM][PF$_6$]					
xIL = 0.25					
1	7.49	0.35	0.15	7.99	93.73
2	6.55	0.20	0.08	6.84	95.81
3	6.37	0.19	0.07	6.64	95.99
4	5.50	0.16	0.06	5.72	96.07
5	5.21	0.15	0.05	5.42	96.23
xIL = 0.50					
1	13.59	0.35	0.15	14.09	96.44
2	10.00	0.20	0.08	9.19	96.88
3	7.57	0.16	0.06	7.79	97.11
4	6.53	0.15	0.05	6.73	96.96
5	5.41	0.15	0.05	5.61	96.36
xIL = 0.75					
1	6.76	0.31	0.14	7.21	93.76
2	6.38	0.19	0.08	6.66	95.85
3	5.80	0.16	0.06	6.02	96.26
4	5.90	0.16	0.06	6.13	96.33
5	5.11	0.15	0.05	5.31	96.15

membrane (ILM). Notably, longer sonication times enhance Li^+ flux through the membranes.

Prolonged sonication diminishes flux rate, primarily attributed to sound attenuation in lower-density media with reduced alkali metal content.[18,38] Ultrasound significantly enhances separation efficiency, surpassing previous findings. The

Table 5 Effect of a feed phase concentration containing equal concentration of chlorine slats of Li, Na, and K with different composite membrane containing supported ILM in PVDF sealed in PVC thin film membrane with a 100 kHz ultrasonic frequency, 50% amplitude and sonication sequence with 120 s sonication time in the presence of different concentration of ILM

Feed ppm	J_{Li} (mg cm^{-2})	J_{Na} (min^{-1} Pa^{-1})	J_K	J_t	S_{Li} (%)
[BMIM][PF$_6$]					
xIL = 0.25					
1000	7.38	0.49	0.17	8.03	91.87
750	5.93	0.51	0.17	6.61	89.69
500	5.52	0.39	0.13	6.04	91.48
250	4.50	0.43	0.15	5.07	88.69
xIL = 0.50					
1000	8.81	0.51	0.17	9.49	92.82
750	7.06	0.46	0.16	7.67	92.00
500	6.89	0.46	0.16	7.51	91.83
250	5.65	0.36	0.13	6.14	92.10
xIL = 0.75					
1000	6.46	0.40	0.14	6.99	92.36
750	5.14	0.33	0.13	5.59	91.85
500	4.82	0.43	0.15	5.39	89.36
250	4.01	0.27	0.11	4.39	91.42
[HMIM][PF$_6$]					
xIL = 0.25					
1000	8.25	0.36	0.13	8.73	94.45
750	6.70	0.43	0.15	7.27	92.11
500	6.06	0.36	0.13	6.54	92.59
250	5.74	0.33	0.13	6.20	92.64
xIL = 0.50					
1000	10.37	0.36	0.13	10.86	95.53
750	7.81	0.33	0.13	8.27	94.49
500	7.93	0.33	0.13	8.38	94.56
250	6.50	0.27	0.11	6.87	94.52
xIL = 0.75					
1000	7.42	0.30	0.12	7.83	94.69
750	6.10	0.27	0.11	6.48	94.18
500	5.82	0.30	0.12	6.23	93.32
250	4.74	0.21	0.09	5.05	93.90
[MOIM][PF$_6$]					
xIL = 0.25					
1000	8.93	0.21	0.09	9.24	96.67
750	7.29	0.23	0.09	7.62	95.70
500	6.42	0.19	0.08	6.70	95.85
250	6.29	0.19	0.08	6.57	95.77
xIL = 0.50					
1000	11.01	0.22	0.09	11.33	97.20
750	8.25	0.19	0.08	8.53	96.74
500	8.74	0.19	0.08	9.01	96.92
250	6.85	0.16	0.07	7.08	96.77
xIL = 0.75					
1000	7.78	0.17	0.08	8.03	96.78
750	6.65	0.16	0.07	6.88	96.67
500	6.25	0.18	0.08	6.52	95.89
250	5.25	0.12	0.06	5.43	96.70

Table 6 The utilized membrane materials for specific brine Li flux and selectivity of Li with respect to the components of the brine with corresponding references

Membrane materials	Water contact angle	Brine	Lithium flux	Selectivity	Reference
PES/[OMIM][PF6]:TBP:PVC–PVP	70	Alkali metal salts 1000 ppm Li, Na, K	Average 13 mg cm^{-2} min^{-1} Pa^{-1}	>95%	This work
QPPO	—	—	0.238 mol m^{-2} h^{-1}	5.92	46
PEI/γ-CDs-TMC	44.5	N/A	4.86 L m^{-2} h^{-1} bar^{-1}	$S_{Li,Mg} = 10.8$	47
IL-modified polyamide	38	$MgCl_2$/LiCl mixtures	26.11 L m^{-2} h^{-1} bar^{-1}	N/A	48
GCS membrane modified by SWCNTs and AB12C4	—	N/A	N/A	Li^+ selectivity: 37.0 mg g^{-1}, separation factors: Na^+ (18.97), K^+ (26.19), Mg^{2+} (16.67), Ca^{2+} (19.64)	49
Ion exchange and bipolar membranes	—	H_3BO_3 and LiOH solutions	45.7×10^{-3} (without ZIF-8), 63×10^{-3} (with ZIF-8)	N/A	50
Polymer inclusion membrane (PIM)	—	Li^+, Na^+, K^+, Ca^{2+}, and Mg^{2+} aqueous solution	45.7×10^{-3} (without ZIF-8), 63×10^{-3} (with ZIF-8)	N/A	51
Dibenzo-14-crown-4 ether-based polyimide (poly(DAB14C4-6FDA))	—	Not specified	—	Li to Na: 45.6, Li to K: 48.3	52
Sodium periodate-oxidized polydopamine	—	200 mg L^{-1} solution of Li^+	—	Li/Mn: 6.71, Li/Co: 5.84*etc.*	53
Heterogeneous ion exchange membranes	—	Aqueous solution	Highest lithium flux: 9.78×10^{-9} mol cm^{-2} s^{-1}	Li^+/Mg^{2+} selectivity: not specified	54
Swelling-embedded cation exchange membranes based on sulfonated poly(ether ether ketone)	—	Not specified	Not specified	Li^+/Mg^{2+} selectivity: not specified	55
Ionic liquid-based polymer inclusion membranes	55.23	Aqueous solutions	Initial flux: 0.89×10^{-6} mol m^{-2} s^{-1}	Li^+/Mg^{2+} selectivity: 2.24	56
MXene nanosheets on hydrophilic PTFE membrane, CEM, ACF electrode	—	Li^+/Co^{2+} mixed solution	Not specified	Separating factor over 6	57
Pristine polyamide thin-film composite (TFC) membrane modified with DABIL	31.16	Concentrated Mg/Li mixtures	Sixfold enhancement compared to unmodified membrane	Li^+/Mg^{2+} selectivity of 26.49	58
Kevlar aramid nanofibers (KANFs) interpenetrating networks of PSSMA and ATTO	47.5	Salt lakes	Not specified	Functional for Li^+/Mg^{2+} separation, excellent anti-scaling performance	59
QPPO, *m*-PTP	—	—	0.48 mol m^{-2} h^{-1}	$\beta Li = 14.1$	60

proposed system outperforms previous methods using ILMs in osmotic tubes. IL content in the ILM phase affects separation rate. Viscous ILs require TBP to balance their effects. High-viscosity media absorb sound, influencing sonic wave propagation. ILM phase properties, including thermodynamic interactions and bulk modulus, govern separation. IL viscosity, sound absorption, ILM phase characteristics, and bulk modulus are crucial factors influencing separation in supported ILM systems. Understanding these parameters leads to improved separation processes.[39]

4.2.2. Effect of concentration gradient. Investigation upon the concentration of the studied aqueous alkali chloride contains useful information about ultrasonic propagation and its effect on particle displacement. The results are given in Table 5. The most effective membrane processing has been achieved using [MOIM][PF_6] with weight fraction of 0.5.

The proposed method exhibits enhanced separation efficiency in concentrated solutions, attributed to higher particle density and faster ultrasonic propagation.[40,41] While conventional membrane separations benefit from higher feed concentrations, the opposite trend is observed in this method.[18,24] This suggests that the effectiveness of ultrasonic-assisted separation diminishes as the feed concentration increases. The interplay between ultrasonic propagation, particle displacement, and solution concentration is complex and requires further investigation.

4.3. Possible mechanism for ultrasonic separation

The propagation of ultrasound waves depends on the characteristics of the media. Ultrasound waves can create turbulence, microstreaming, and localized high shear forces that accelerate mass transfer of solutes to the boundary of the membrane phase, facilitating separation.[42] Ultrasound waves can also generate heat in the medium, which may require cooling of the system during sonication. The specific details and outcomes of the ultrasound-mediated mass and heat transfer processes can vary depending on the experimental setup, the properties of the media, and the separation objectives.[43] Further investigation and experimentation are typically necessary to understand the intricacies of these processes and optimize the system for efficient separation.[44] The characteristics of the media, such as sound speed and attenuation, directly impact the propagation of ultrasound waves and their behavior within the system. Cavitation, the formation and collapse of microscopic bubbles, can significantly enhance mass transfer by creating turbulence and disrupting concentration gradients, accelerating the transfer of solutes to the membrane phase. Once at the membrane, the transportation of solutes to the receiver phase is influenced by factors like concentration gradients, diffusion, and membrane properties. Applying ultrasound also generates heat that may require cooling to maintain optimal conditions. The specific outcomes of these ultrasound-driven mass and heat transfer processes can vary based on the experimental setup, media properties, and separation objectives, requiring further investigation to understand and optimize the system.[45]

4.4. Comparison of the results with literature

The literature that used membranes for separation of lithium from brine has been presented in Table 6.

The pristine polyamide thin-film composite (TFC) membrane modified with DABIL exhibited the highest lithium ion selectivity of 26.49 among the membranes studied.[49] The MXene nanosheets on hydrophilic PTFE membrane exhibited a separating factor over 6 for Li^+/Co^{2+} separation.[57] The dibenzo-14-crown-4 ether-based polyimide (poly(DAB14C4-6FDA)) exhibited good selectivity for lithium ions over sodium and potassium ions.[52] Exhibited selectivity for lithium over other transition metals (Li/Mn, Li/Co) present in spent lithium-ion battery leachate. This highlights its potential application in lithium-ion battery recycling.[51] Functional for separating lithium from magnesium, with excellent anti-scaling properties. This characteristic is crucial for long-term membrane performance.[59]

5. Conclusion

A new method for lithium separation with ultrasonic-treated composite membranes including PES sealed with PVC-PVP membrane and identified a key membrane composition (xIL = 0.5 of [MOIM][PF_6]:TBP) for better lithium selectivity. Optimum ultrasonic treatment involved moderate sonication time and a frequency matching the membrane's bulk modulus (250 kHz). Furthermore, higher lithium flux and selectivity were achieved at higher feed concentrations (250 ppm to 1000 ppm).

Data availability

Data are available upon request from the authors.

Conflicts of interest

There are no conflicts to declare.

Acknowledgements

Authors are grateful for grant support of University of Tabriz.

References

1 Y. Fan, H. Li, C. Lu, S. Chen, Y. Yao, H. He, S. Ma, Z. Peng and K. Shao, *J. Clean. Prod.*, 2023, **417**, 138043.
2 J. Qing, X. Wu, L. Zeng, W. Guan, Z. Cao, Q. Li, M. Wang, G. Zhang and S. Wu, *J. Clean. Prod.*, 2023, 139645.
3 P. Fröhlich, T. Lorenz, G. Martin, B. Brett and M. Bertau, *Angew. Chem., Int. Ed.*, 2017, **56**, 2544–2580.
4 H. Gu, T. Guo, H. Wen, C. Luo, Y. Cui, S. Du and N. Wang, *Miner. Eng.*, 2020, **145**, 106076.
5 L. Kölbel, T. Kölbel, L. Herrmann, E. Kaymakci, I. Ghergut, A. Poirel and J. Schneider, *Hydrometallurgy*, 2023, **221**, 106131.
6 S. Chen, Y. Dong, J. Sun, P. Gu, J. Wang and S. Zhang, *Green Chem.*, 2023, **25**, 5813–5835.
7 X. Cheng, Q. Pan, H. Tan, K. Chen, W. Liu, Y. Shi, S. Du and B. Zhu, *RSC Adv.*, 2023, **13**, 22113–22121.

8 A. M. Bradshaw and T. Hamacher, *ChemSusChem*, 2012, **5**, 550–562.
9 V. Flexer, C. F. Baspineiro and C. I. Galli, *Sci. Total Environ.*, 2018, **639**, 1188–1204.
10 Y. J. Lim, K. Goh, A. Goto, Y. Zhao and R. Wang, *J. Mater. Chem. A*, 2023, **11**, 22551–22589.
11 Ö. Tekinalp, P. Zimmermann, S. Holdcroft, O. S. Burheim and L. Deng, *Membranes*, 2023, **13**, 566.
12 S. Xiong, X. Qian, Z. Zhong and Y. Wang, *J. Membr. Sci.*, 2022, **658**, 120740.
13 C. Wang, J. Tang, Z. Chen, Y. Jin, J. Liu, H. Xu, H. Wang, X. He and Q. Zhang, *Energy Storage Mater.*, 2023, **55**, 498–516.
14 T. Zhou, C. Gui, L. Sun, Y. Hu, H. Lyu, Z. Wang, Z. Song and G. Yu, *Chem. Rev.*, 2023, **123**(21), 12170–12253.
15 H. Jo, T.-H. Le, H. Lee, J. Lee, M. Kim, S. Lee, M. Chang and H. Yoon, *Chem. Eng. J.*, 2023, **452**, 139274.
16 T. Zhang, W. Zheng, Q. Wang, Z. Wu and Z. Wang, *Desalination*, 2023, **546**, 116205.
17 P. Kallem, N. Elashwah, G. Bharath, H. M. Hegab, S. W. Hasan and F. Banat, *ACS Appl. Nano Mater.*, 2023, **6**, 607–621.
18 H. Shekaari and B. Golmohammadi, *Ultrason. Sonochem.*, 2021, **74**, 105549.
19 M. K. Shahid, A. Kashif, P. R. Rout, M. Aslam, A. Fuwad, Y. Choi, R. Banu J, J. H. Park and G. Kumar, *J. Environ. Manage.*, 2020, **270**, 110909.
20 I. Lenart and D. Ausländer, *Ultrasonics*, 1980, **18**, 216–218.
21 L. Beranek and T. Mellow, in *Acoustics: Sound Fields, Transducers and Vibration*, Elsevier, 2019, pp. 25–79.
22 M. Long, in *Architectural Acoustics*, Elsevier, 2014, pp. 221–258.
23 F. Fahy, in *Foundations of Engineering Acoustics*, Elsevier, 2001, pp. 23–47.
24 G. Zante, M. Boltoeva, A. Masmoudi, R. Barillon and D. Trébouet, *J. Membr. Sci.*, 2019, **580**, 62–76.
25 X. Yan, S. Anguille, M. Bendahan and P. Moulin, *Sep. Purif. Technol.*, 2019, **222**, 230–253.
26 I. Vázquez-Fernández, A. Bouzina, M. Raghibi, L. Timperman, J. Bigarré and M. Anouti, *J. Mater. Sci.*, 2020, **55**, 16697–16717.
27 T. T. V. Tran, C. H. Nguyen, W.-C. Lin and R.-S. Juang, *Sep. Purif. Technol.*, 2021, **277**, 119615.
28 Y. Mi and X. Yu, *J. Sound Vib.*, 2020, **489**, 115679.
29 G. Zhou, J. H. Wu, K. Lu, X. Tian, W. Huang and K. Zhu, *Appl. Acoust.*, 2020, **159**, 107078.
30 R. Zhang, Y. Huang, C. Sun, L. Xiaozhen, X. Bentian and Z. Wang, *Ultrason. Sonochem.*, 2019, **55**, 341–347.
31 H. Delmas, L. Barthe and R. Cleary, in *Power Ultrasonics*, ed. J. A. Gallego-Juárez, K. F. Graff and M. Lucas, Woodhead Publishing, edn.2nd, 2023, pp. 665–685.
32 J. Wu, *Fluids*, 2018, **3**, 108.
33 M. Singla and N. Sit, *Ultrason. Sonochem.*, 2021, **73**, 105506.
34 D. Radziuk and H. Möhwald, *Phys. Chem. Chem. Phys.*, 2016, **18**, 21–46.
35 S. M. Chowdhury, L. Abou-Elkacem, T. Lee, J. Dahl and A. M. Lutz, *J. Controlled Release*, 2020, **326**, 75–90.
36 L. Borea, V. Naddeo, M. S. Shalaby, T. Zarra, V. Belgiorno, H. Abdalla and A. M. Shaban, *Ultrasonics*, 2018, **83**, 42–47.
37 D. Radziuk and H. Möhwald, *ChemPhysChem*, 2016, **17**, 931–953.
38 M. Amarillo, N. Pérez, F. Blasina, A. Gambaro, A. Leone, R. Romaniello, X.-Q. Xu and P. Juliano, *Ultrason. Sonochem.*, 2019, **53**, 142–151.
39 S. L. Nedelec, J. Campbell, A. N. Radford, S. D. Simpson and N. D. Merchant, *Methods Ecol. Evol.*, 2016, **7**, 836–842.
40 D. J. Collins, Z. Ma and Y. Ai, *Anal. Chem.*, 2016, **88**, 5513–5522.
41 T. Leong, L. Johansson, P. Juliano, S. L. McArthur and R. Manasseh, *Ind. Eng. Chem. Res.*, 2013, **52**, 16555–16576.
42 B. Khadhraoui, V. Ummat, B. K. Tiwari, A. S. Fabiano-Tixier and F. Chemat, *Ultrason. Sonochem.*, 2021, **76**, 105625.
43 M. Chiha, O. Hamdaoui, F. Ahmedchekkat and C. Pétrier, *Ultrason. Sonochem.*, 2010, **17**, 318–325.
44 Y. Yao, Y. Pan and S. Liu, *Ultrason. Sonochem.*, 2020, **62**, 104722.
45 B. Golmohammadi and H. Shekaari, *Ultrason. Sonochem.*, 2024, **108**, 106974.
46 X. Zeng, L. Xu, T. Deng, Y. Wang, W. Xu and W. Zhang, *ACS Sustainable Chem. Eng.*, 2023, **11**, 12877–12887.
47 Y. Zhao, N. Li, J. Shi, Y. Xia, B. Zhu, R. Shao, C. Min, Z. Xu and H. Deng, *Sep. Purif. Technol.*, 202, **286**, 120419.
48 F. Soyekwo, H. Wen, D. Liao and C. Liu, *J. Membr. Sci.*, 2022, **659**, 120773.
49 M. Cheng, T. Chu, X. Yin, S. Hou and Y. Yang, *ACS Sustainable Chem. Eng.*, 2022, **10**, 12613–12619.
50 Y. A. Jarma, E. Çermikli, D. İpekçi, E. Altıok and N. Kabay, *Desalination*, 2021, **500**, 114850.
51 H. Kazemzadeh, J. Karimi-Sabet, J. Towfighi Darian and A. Adhami, *Sep. Purif. Technol.*, 2020, **251**, 117298.
52 Q. Zhu, X. Ma, H. Pei, J. Li, F. Yan, Z. Cui, H. Wang and J. Li, *Sep. Purif. Technol.*, 2020, **247**, 116940.
53 Z. Li, G. He, G. Zhao, J. Niu, L. Li, J. Bi, H. Mu, C. Zhu, Z. Chen, L. Zhang, H. Zhang, J. Zhang, B. Wang and Y. Wang, *Sep. Purif. Technol.*, 2021, **277**, 119519.
54 D. İpekçi, N. Kabay, S. Bunani, E. Altıok, M. Arda, K. Yoshizuka and S. Nishihama, *Desalination*, 2020, **479**, 114313.
55 H. Qian, G. Xu, S. Yang, E. H. Ang, Q. Chen, C. Lin, J. Liao and J. Shen, *ACS Appl. Mater. Interfaces*, 2024, **16**, 18019–18029.
56 L. Xu, X. Zeng, Q. He, T. Deng, C. Zhang and W. Zhang, *Sep. Purif. Technol.*, 2022, **288**, 120626.
57 L. Jiang, L. Zhu, L. Chen, Y. Ding, W. Zhang and S. Brice, *Sep. Purif. Technol.*, 2022, **302**, 122082.
58 F. Soyekwo, H. Wen, D. Liao and C. Liu, *ACS Appl. Mater. Interfaces*, 2022, **14**, 32420–32432.
59 Y. Zhao, M. Wu, P. Shen, C. Uytterhoeven, N. Mamrol, J. Shen, C. Gao and B. Van der Bruggen, *J. Membr. Sci.*, 2021, **618**, 118668.
60 G. Luo, Y. Wu, X. Zeng, W. Zhou, P. Wang and W. Zhang, *ACS Appl. Mater. Interfaces*, 2024, DOI: **10.1021/acsami.3c19100**.